# Preferential Site of Attack on Fullerene Cations: Frontier Orbitals and Rate Coefficients

**Kee Hag Lee,*,†,‡ Changhoon Lee,† Jinhee Kang,† Sung Soo Park,# Jeeyoung Lee,† Sang Kuk Lee,§ and Diethard K. Bohme*,||**

*Department of Chemistry and Research Institute of Basic Sciences, Wonkwang University, Iksan, Jeonbuk 570-749, S. Korea, CAE Group, Central R & D Institute, Samsung Electro-Mechanics Co. Ltd., Suwon 443-803, Korea, Department of Chemistry, Pusan National University, Pusan 609-735, S. Korea, Department of Chemistry, York University, Toronto, Ontario, Canada M3J 1P3, and Department of Material Science and Engineering, Cornell University, 214 Bard Hall, Ithaca, New York 14853-1501*

*Received: August 15, 2006*

An analysis of reaction efficiency is presented for reactions of carbonaceous ions and molecules. Our results show that the combination of experimental rate-coefficient measurements and computations of the condensed Fukui functions of frontier molecular orbitals and pyramidal angles of $\pi$ orbitals is very useful for elucidating the reactive sites on fullerene carbon clusters in the gas phase.

## 1. Introduction

In comparison with normal planar conjugated organic molecules, the fullerenes greatly favor reactions that decrease strain, whereas those reactions that increase strain are inhibited.[1] Fullerene molecules and their ions provide a range of reactive C sites with different degrees of hybridization and strain.[1,2] Nucleophilic addition[3−5] and cycloaddition[6] to $C_{70}$ favor the carbon atoms which have the most pyramidal shape (sites 1 and 2 in Figure 1). Meanwhile, the preferential electrophilic attack[7] of $C_{70}$ recently observed under Friedel−Crafts conditions ($CHCl_3/AlCl_3$) favors the less pyramid site of $C_{70}$ (site 4 in Figure 1). Solution studies of the osmylation of $C_{70}$ have identified regioselectivity with different surface strain.[8] Osmylation occurs mainly at the bond between highly pyramidalized carbons, to a lesser extent at the bond between carbons pyramidalized like those in $C_{60}$, and little or not at all at the bond between the less pyramidalized carbons.

Investigations with a selected-ion flow tube (SIFT) tandem mass spectrometer[9] of addition reactions of $C_{56}^+$, $C_{58}^+$, and $C_{60}^+$ with $NH_3$, $C_{56}^{2+}$, $C_{58}^{2+}$, and $C_{60}^{2+}$ with $C_2H_2$ and $CH_3CN$, and hydride-transfer reactions[10] of $C_{56}^{2+}$, $C_{58}^{2+}$, and $C_{60}^{2+}$ with $n$-$C_4H_{10}$ revealed an enhanced reactivity for the adjacent-pentagon fullerene ions of $C_{56}$ and $C_{58}$ compared to those of $C_{60}$. Adjacent pentagons enhance the curvature of the carbon surface of selected C sites.[10] Also, systematic experimental studies of gas-phase addition reactions of $C_{56}^+$, $C_{58}^+$, $C_{60}^+$, $C_{70}^+$, corannulene$^+$, and coronene$^+$ with cyclopentadiene and 1,3-cyclohexadiene[11] have shown that the efficiency of bond formation with these two molecules also depends strongly on the curvature of the carbonaceous surface of the reacting cation.[2,11] For example, the Diels−Alder addition of cyclopentadiene[11] is faster with the smaller, more strained fullerene cations, and the efficiencies of addition to the less strained corannulene cation and the flat coronene cation are immeasurably small. Since this order of reactivity follows the relative magnitudes of the $\pi$-orbital axis vector (POAV) angles, the gas-phase experiments suggest that POAV angles provide a very useful guide for understanding the measured reaction efficiencies.

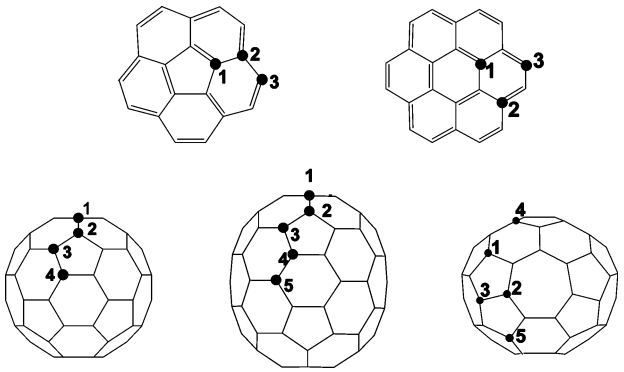


**Figure 1.** Numbered carbon sites in corannulene, coronene, $C_{60}$, $C_{70}$, and $C_{58}$. See Table 1 for the magnitude of the $\pi$-orbital axis vector (POAV) angle at each site for these molecules and their cations.

The $\pi$-orbital axis vector (POAV) is defined as that vector which makes equal angles ($\theta_{\sigma\pi}$) to the three $\sigma$-bonds at a conjugated carbon atom.[1] The POAV angle $= (\theta_{\sigma\pi} - 90°)$ (see Scheme 1) and is 0° and 19.37° for a planar $sp^2$ and a tetrahedral $sp^3$ carbon atom, respectively. Table 1 provides a summary of the different POAV angles at the sites of the molecules shown in Figure 1 and their cations. $C_{60}$ has only one such site, while $C_{70}$ has five different types of C sites with different surface strain. The bowl-shaped corannulene molecule has three types of C sites including one without strain, whereas there is no strain in the flat PAH coronene. The corresponding cations have a reduced symmetry except $C_{70}$. The $I_h$ symmetry of the neutral $C_{60}$ reduces to the $D_{5d}$ symmetry in its cation which has four distinguishable sites.

The POAV analysis of hybridization also has been introduced as a unifying metric for the degree of structural progress in an organic reaction.[12] Here, we extend this concept to find the reaction site (which has a specific POAV angle) from a knowledge of the reaction efficiency. We apply ab initio quantum chemical methods and obtain the frontier function from electronic properties of the highest occupied molecular orbital

* Authors to whom correspondence should be addressed. E-mail: (K.L.) khlee@wonkwang.ac.kr and (D.B.) dkbohme@yorku.ca.
† Wonkwang University.
‡ Cornell University.
# Samsung Electro-Mechanics Co. Ltd.
§ Pusan National University.
|| York University.

10.1021/jp0652749 CCC: $33.50 
Published on Web 09/19/2006

**SCHEME 1: POAV Pyramidalization Angle [($\theta_{\sigma\pi}$ − 90°), Deg]**

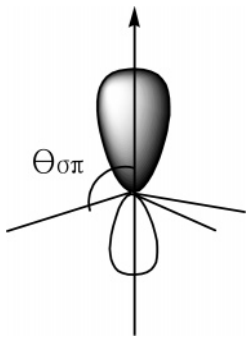


**TABLE 1: POAV Angles for Various Sites on Selected Carbonaceous Molecules (and Their Cations) and the Indices (×10³) of the Condensed Fukui Function of Their Cations in Optimized Structures at the Level of B3LYP/6-31G*** [a]

| sites | $C_{60}$ | $C_{70}$ | $C_{58}$ | corannulene | coronene |
|---|---|---|---|---|---|
| 1 | 11.6 | 11.9 | 15.2 | 8.1 | 0 |
| | (11.7) | (11.7) | (14.6) | (7.5) | (0) |
| | 16 | 14 | 33 | 32 | 17 |
| 2 | 11.6 | 11.9 | 12.7 | 3.7 | 0 |
| | (11.8) | (12.0) | (12.2 | (3.3) | (0) |
| | 16 | 15 | 25 | 23 | 23 |
| 3 | 11.6 | 11.4 | 15.5 | 1.6 | 0 |
| | (11.7) | (11.5) | (15.7) | (1.8) | (0) |
| | 14 | 14 | 23 | 21 | 35 |
| 4 | 11.6 | 10.2 | 11.3 | | |
| | (11.4) | (10.2) | (10.8) | | |
| | 20 | 17 | 21 | | |
| 5 | | 8.7 | 12.0 | | |
| | | (8.7) | (11.7) | | |
| | | 9 | 20 | | |

[a] The top number is the POAV angle for the neutral, the number in parentheses is the POAV angle for the cation, and the lowest number is the index of the condensed Fukui function for the cation.

(HOMO) and the lowest unoccupied molecular orbital (LUMO). The POAV should be more useful for predicting the preferred site of attack in these reactions' angle in combination with the frontier function. The frontier function or Fukui function[13] of chemical reactivity is a local quantity, which has different values at different sites of a molecule. The preferred site of chemical attack is the site with the largest frontier function. The condensed Fukui function is obtained with hybrid density fuctional theory.

## 2. Calculations

The structures of the corannulene, coronene, $C_{60}$, $C_{70}$, $C_{58}$, and their cations were optimized with the density functional method (using 6-31G* basis sets) using Becke's three-parameter hybrid method and the Lee−Yang−Parr correlation functional (B3LYP).[14] All geometries at local minima are fully optimized using the Gaussian 03 suite of programs.[15] Our discussion is based mostly on B3LYP/6-31G*//B3LYP/6-31G* (B3LYP/6-31G*) results. The structures that were studied here at the level of B3LYP/6-31G* are those shown in Figure 1. The POAV analysis of the geometrical structures was carried out with the POAV3 program, which is available from QCPE.[16]

## 3. Results and Discussion

The $I_h$ symmetry of the neutral $C_{60}$ is reduced to $D_{5d}$ symmetry in its cation in our calculations. $C_{70}$ has the same symmetry, $D_{5h}$, for both the neutral and its cation. Table 1 gives the POAV angles for various sites on the optimized structures

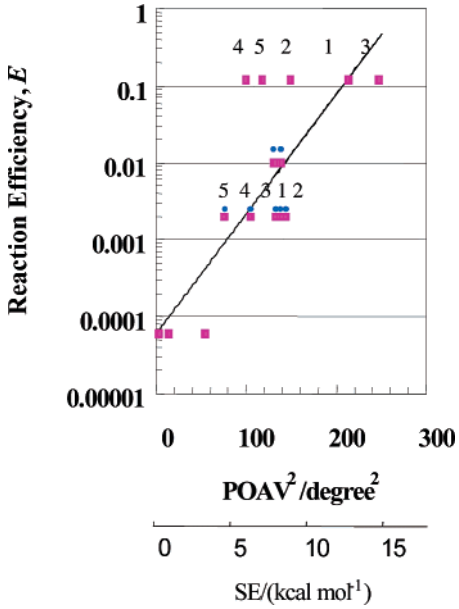


**Figure 2.** Semilogarithmic plot for the dependence of reaction efficiency ($E$) on the square of the $\pi$-orbital axis vector (POAV) angle for reactions of various carbonaceous cations with cyclopentadiene (squares) and 1,3-cyclohexadiene (circles) in He buffer gas. $E = k_{obs}/k_c$, where $k_{obs}$ is the measured rate coefficient and $k_c$ is the collision rate coefficient, which is estimated to be $10^{-9}$ cm$^3$ molecule$^{-1}$ s$^{-1}$. The numbers of the distinguishable sites are indicated for $C_{58}^+$ and $C_{70}^+$.

of selected carbonaceous molecules and their cations at the level of B3LYP/6-31G*. The POAV angles of coronene and its cation are 0°. Table 1 also includes values for the four and five different carbon sites for $C_{60}^+$ and $C_{70}^+$ with structural symmetries of $D_{5d}$ and $C_{5h}$, respectively. Corrannulene has three different carbon sites in its $C_{5v}$ symmetry. However, its cation has $C_s$ symmetry. Table 1 lists the three carbon sites with the largest Fukui functions. For $C_{58}$ which has $C_s$ symmetry, Table 1 provides POAV angles for the five sites (among thirty-one different sites) that have larger coefficients in the HOMO and LUMO than the others.

Figure 2 shows a semilogarithmic plot of the dependence of the previously reported experimental reaction efficiency ($E$) on the square of the $\pi$-orbital axis vector angle for reactions of various carbonaceous cations with cyclopentadiene and 1,3-cyclohexadiene.[2,11] Here, $E$ is defined as $k_{obs}/k_c$, where $k_{obs}$ is the measured rate coefficient and $k_c$ is the collision rate coefficient, which is estimated to be $10^{-9}$ cm$^3$ molecule$^{-1}$ s$^{-1}$.[2,11] This plot is drawn on eq 1, which is derived from the experimental data of the reaction efficiency as a function of POAV angles at carbon sites with the largest values of indices of the condensed Fukui function[13] of selected carbonaceous surfaces at the level of the hybrid density functional (B3LYP/6-31G*) method,

$$k_{obs} = 6.0 \times 10^{-14} e^{0.60SE} \quad \text{where} \quad SE = 196(\theta - \pi/2)^2 \tag{1}$$

Here, SE is the strain energy[17] at a given carbon atom in kcal mol$^{-1}$, where $\theta$ is the POAV angle in radians. The square of the relation coefficient is 0.999. Equation 1 intercepts the most reactive sites as predicted by the condensed Fukui functions and so should be useful for predicting the reaction sites of other fullerenes.

Figure 2 and eq 1 suggest that the reactions of the $C_{58}^+$ and the $C_{70}^+$ cations occur at sites 1 and 4, respectively, of five different carbon sites. These are the sites with the highest indices

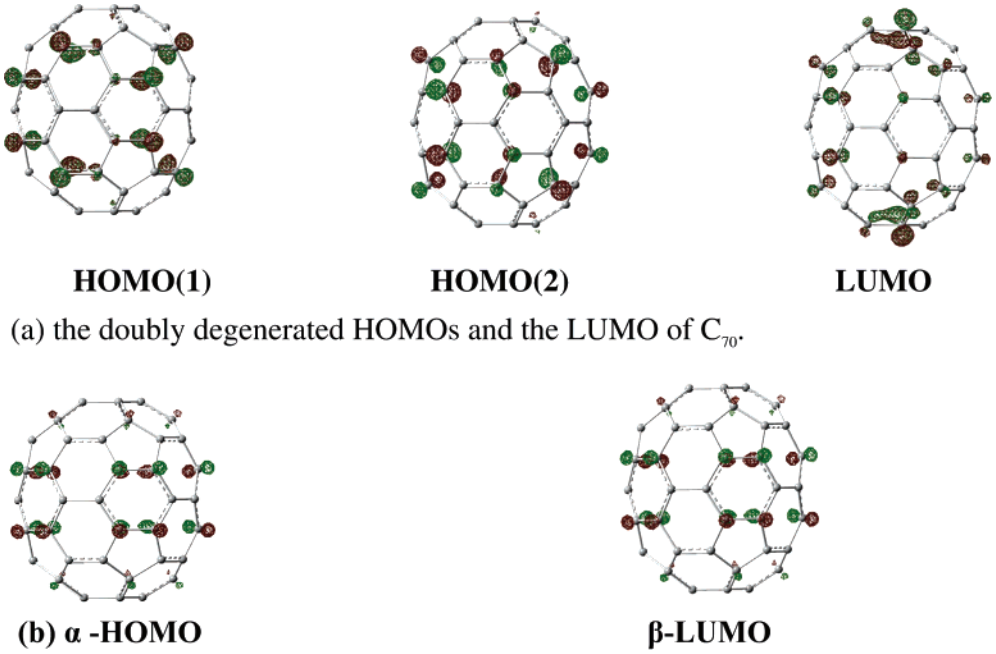


**Figure 3.** HOMO and LUMO of the $C_{70}$ molecule (a) and its cation (b).

**SCHEME 2: Different Orbital Characters at Different Geometrical Environments of Carbon Atoms**

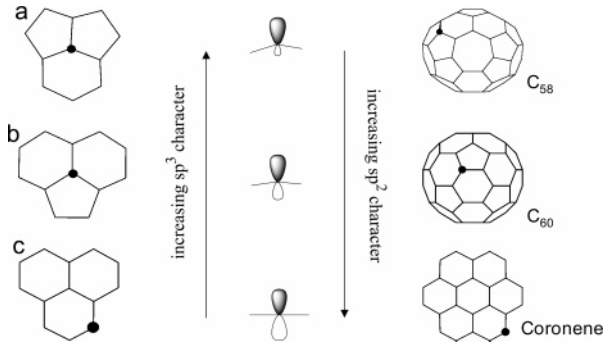


of the condensed Fukui functions, and this leads to the important result that the measured rate coefficients (or reaction efficiencies) are useful for confirming the reaction and bonding sites on surfaces of fullerene cations in the gas phase. This preferred reactive site is in line with the lowest energy structure of the alkylated $C_{70}$ cation which was confirmed by NMR measurements and DFT calculations of the relative energies of regioisomers of alkylated $C_{70}$ cation.[7] Scheme 2 shows the qualitative orbital character at the reaction sites in Table 1. These also suggest that the preference for reaction at a particular C site is not only a function of the highest strain energy (which is the site with the highest local curvature) in those cations by the relief of strain energy but is also a function of the frontier electronic structure of the chemical species.

Scheme 2 is an illustration of different environments for carbon atoms. The formation of a fourth chemical bond to a carbon atom, in a tetrahedral coordination, implies $sp^3$ hybridization at the carbon concerned in the resulting product. This process is expected to be easiest at sites that already feature a high degree of $sp^3$ character.

Figure 3 shows the HOMO and LUMO for various sites on $C_{70}$ molecule and its cation at the level of B3LYP/6-31G*. The large LUMO coefficients (Figure 3a) predict that the preferential nucleophilic attack of $C_{70}$ occurs at sites 1 and 2, which have the most pyramidal shape. Meanwhile, the preferential carbon site for electrophilic attack of $C_{70}$ is not clear in the HOMO of neutral $C_{70}$, which shows a doubly degenerate state and competition between 6−6 and 5−6 ring junctions. Thus, although the LUMO of the cation could be inferred from the HOMO of $C_{70}$,[7] caution should be exercised if the degenerate HOMO of the neutral is split in the LUMO of its cation.

Figure 3b shows that the HOMO and LUMO for $C_{70}^+$ have the identical orbital character because the $C_{70}$ molecule and its cation have the same symmetry and the HOMO of the $C_{70}$ molecule is degenerate. The α-HOMO of its cation apparently shows the electrophilic sites of attack of $C_{70}^+$ that control the addition to the bond common to adjacent five- and six-membered rings. Also, the $\beta$-LUMO of its cation clearly shows the nucleophilic sites of attack of $C_{70}^+$ that control the addition to the bond common to adjacent five- and six-membered rings. Meier and co-workers already reported that addition of benzyne to $C_{70}$ produces four adducts, one of which resulted from the addition to such a bond.[6b] Site 4 and its nearest neighbor sites (see the sites of $C_{70}$ in Figure 1) have bonding character because they have the same lobe direction. These are in line with the predictions made here on the basis of the condensed Fukui function and the POAV angle.

Therefore, our analysis of reaction efficiency shows that the combination of experimental SIFT rate-coefficient measurements and computations of the condensed Fukui functions and POAV angles is very useful for elucidating the reactive sites on fullerene carbon clusters in the gas phase. Also, as far as we know, this is the first demonstration of the combined influence of an electronic effect (the condensed Fukui function) and a geometric effect (the POAV angle) in determining the progress of reactions involving fullerene clusters.

**Acknowledgment.** This work was supported by the Korea Research Foundation Grant (KRF-2003-015-C00261), in which main calculations were performed by using the supercomputing resources of the Korea Institute of Science and Technology Information (KISTI), and by the BK21 Program of the Ministry of Education and Human Resources Development of Korea. This work (to S.K.L.) was also supported by grant No. (R01-2005-000-10582-0) from the Basic Research Program of the Korea

Science & Engineering Foundation. One of us (K.H.L.) would like to thank Prof. Roald Hoffmann for his warm comment on this paper.

## References and Notes

(1) Haddon, R. C. *Science (Washington, D.C.)* **1993**, *261*, 1545.

(2) Bohme, D. K. *Can. J. Chem.* **1999**, *77*, 1453.

(3) Sawamura, M.; Iikura, H.; Hirai, A.; Nakamura, E. *J. Am. Chem. Soc.* **1998**, *120*, 8285.

(4) Thilgen, C.; Herrmann, A.; Diederich, F. *Angew. Chem., Int. Ed. Engl.* **1997**, *36*, 2268.

(5) Wang, Z.; Meier, M. S. *J. Org. Chem.* **2004**, *69*, 2178.

(6) (a) Bellavia-Lund, C.; Wudl, F. *J. Am. Chem. Soc.* **1997**, *119*, 943. (b) Meier, M. S.; Wang, G.-W.; Haddon, R. C.; Brock, C. P.; Lloyd, M. A.; Selegue, J. P. *J. Am. Chem. Soc.* **1998**, *120*, 2337.

(7) Kitagawa, K.; Lee, Y.; Masaoka, N.; Komatsu, K. *Angew. Chem., Int. Ed.* **2005**, *44*, 1398.

(8) Hawkins, J. M.; Meyer, A.; Solow, M. A. *J. Am. Chem. Soc.* **1993**, *115*, 7499.

(9) Raksit, A. B.; Bohme, D. K. *Int. J. Mass. Spectrom. Ion Processes* **1983/1984**, *55*, 69. Mackay, G. I.; Vlachos, G. D.; Bohme, D. K.; Schiff, H. I. *Int. J. Mass Spectrom. Ion Phys.* **1980**, *36*, 259.

(10) Petrie, S.; Bohme, D. K. *Nature (London)* **1993**, *365*, 426.

(11) Becker, H.; Scott, L. T.; Bohme, D. K. *Int. J. Mass. Spectrom. Ion Processes* **1997**, *167/168*, 519.

(12) Haddon, R. C.; Chow, S.-Y. *J. Am. Chem. Soc.* **1988**, *110*, 10494. Haddon, R. C.; Chow, S.-Y. *Pure Appl. Chem.* **1999**, *71*, 289.

(13) Parr, R. G.; Yang, W. *J. Am. Chem. Soc.* **1984**, *106*, 4049. Castellano, E. E.; Piro, O. E.; Caram, J. A.; Mirifico, M. V.; Aimone, S. L.; Vasini, E. J.; Marquez-Lucero, A.; Glossman-Mitnik, D. *J. Mol. Struct. (THEOCHEM)* **2001**, *597*, 163. Tiznado, W.; Chamorro, E.; Contreras, R.; Fuentealba *J. Phys. Chem. A* **2005**, *109*, 3220.

(14) Becke, A. D. *J. Chem. Phys.* **1993**, *98*, 5648. Lee, C.; Yang, W.; Parr, R. G. *Phys. Rev. B* **1988**, *37*, 785.

(15) Frisch, M. J.; Trucks, G. W.; Schlegel, H. B.; Scuseria, G. E.; Robb, M. A.; Cheeseman, J. R.; Montgomery, J. A., Jr.; Vreven, T.; Kudin, K. N.; Burant, J. C.; Millam, J. M.; Iyengar, S. S.; Tomasi, J.; Barone, V.; Mennucci, B.; Cossi, M.; Scalmani, G.; Rega, N.; Petersson, G. A.; Nakatsuji, H.; Hada, M.; Ehara, M.; Toyota, K.; Fukuda, R.; Hasegawa, J.; Ishida, M.; Nakajima, T.; Honda, Y.; Kitao, O.; Nakai, H.; Klene, M.; Li, X.; Knox, J. E.; Hratchian, H. P.; Cross, J. B.; Adamo, C.; Jaramillo, J.; Gomperts, R.; Stratmann, R. E.; Yazyev, O.; Austin, A. J.; Cammi, R.; Pomelli, C.; Ochterski, J. W.; Ayala, P. Y.; Morokuma, K.; Voth, G. A.; Salvador, P.; Dannenberg, J. J.; Zakrzewski, V. G.; Dapprich, S.; Daniels, A. D.; Strain, M. C.; Farkas, O.; Malick, D. K.; Rabuck, A. D.; Raghavachari, K.; Foresman, J. B.; Ortiz, J. V.; Cui, Q.; Baboul, A. G.; Clifford, S.; Cioslowski, J.; Stefanov, B. B.; Liu, G.; Liashenko, A.; Piskorz, P.; Komaromi, I.; Martin, R. L.; Fox, D. J.; Keith, T.; Al-Laham, M. A.; Peng, C. Y.; Nanayakkara, A.; Challacombe, M.; Gill, P. M. W.; Johnson, B.; Chen, W.; Wong, M. W.; Gonzalez, C.; Pople, J. A. *Gaussian 03*, Revision B.05; Gaussian, Inc.: Pittsburgh, PA, 2003.

(16) Haddon, R. C. QCPE 508/QCMP044, POAV3. http://qcpe.chem.indiana.edu.

(17) Haddon, R. C.; Raghavachari, K. *Tetrahedron* **1996**, *52*, 5207.